Journal of Applied Electrochemistry **32**: 415–424, 2002.

Recycling wood pulping chemicals by molten salt electrolysis: cyclic voltammetry of mixtures containing Na_2CO_3 and Na_2SO_4

R. WARTENA[1], J. WINNICK[1]* and P.H. PFROMM[2]*†
[1]*School of Chemical Engineering, Georgia Institute of Technology, Atlanta, GA 30332, USA*
[2]*Institute of Paper Science and Technology, Atlanta, GA 30318, USA*
*(*authors for correspondence)*
(†Presently at: Department of Chemical Engineering, Kansas State University, Manhattan, Kansas, 66506-5102, USA)

Received 4 June 2001; accepted in revised form 22 January 2002

Key words: carbonate, causticizing, kraft process, pulping

Abstract

We are investigating a novel electrochemical pathway for efficient recycling of inorganic chemicals from the kraft pulping process. To analyse this process, cyclic voltammetry was conducted on molten salts containing sodium carbonate, or sodium carbonate and sodium sulfate on gold and nickel/nickel oxide electrodes. Pure sodium carbonate at 860 °C was determined to exhibit oxidation to carbon dioxide and oxygen. Electrochemical reduction proceeded to both sodium metal and to sodium oxide and either carbon or carbon monoxide. A mixture with a 2.36:1 molar ratio of sodium carbonate to sodium sulfate at 860 °C was investigated where the anode again displayed carbonate oxidation. The cathode reactions are the reduction of sulfate ions to form sulfide and oxide ions and carbonate reduction to oxide ions and carbon monoxide. Separated cell operation to avoid oxide ion oxidation appears necessary according to the cyclic voltammetry. Nickel oxide was found to be a stable anode material in a sodium carbonate molten salt. This paper, based on cyclic voltammetry results of oxide ion production, is the first step towards a technical electrolysis process for recausticizing of molten smelt for the kraft pulping process.

1. Introduction

1.1. *Application to the pulp and paper industry*

The overall goal of this work is to arrive at an electrochemical molten salt process as an alternative to the traditional equilibrium-limited wet chemical method [1] for causticizing a kraft smelt. More than 50 million tons of kraft pulp are produced in the US per year [2]. The recovery and recycling of the inorganic chemicals needed in the kraft process (active pulping chemicals are NaOH and Na_2S, spent chemicals to be recycled are mainly sodium sulfate and sodium carbonate) is one of the significant inorganic chemical operations in the US, amounting to processing of about 25 million tons of inorganic molten salt (termed kraft smelt) per year. The motivation for the work shown here is a concept for an electrochemical process that could supply incremental recausticizing capacity to pulp mills (both through reduced deadload and incremental chemical recovery capacity), improved energy efficiency, reduced introduction of contaminants into the process, and simplified operation (shortened holdup time, elimination of multiple equilibrium limited chemical reaction/separation steps, elimination of the cumbersome lime cycle involving a kiln).

The kraft process uses an aqueous mixture of sodium hydroxide and sodium sulfide at elevated temperature and pressure to liberate the valuable cellulose fibers from wood. The waste product is 'black liquor', an aqueous mixture predominately containing sodium carbonate (Na_2CO_3), sodium sulfate (Na_2SO_4) and sodium sulfide (Na_2S), in addition to organic material removed form the wood during pulping. A molten salt mixture containing mainly sodium carbonate, sodium sulfide and sodium sulfate is recovered continuously at 750–900 °C from the bottom of the recovery furnace which combusts the organics in black liquor. The recovery furnace converts a large portion of the sodium sulfate (spent chemical) to sodium sulfide (needed pulping chemical) due to reducing conditions in certain parts of the furnace. The composition of the molten salt leaving the recovery furnace (Na_2CO_3:[Na_2S + Na_2SO_4]) ranges generally from 1:1 to 4:1 (molar basis) [3].

The traditional chemical recovery process starts with dissolution of the molten salts (kraft smelt) in water followed by a chemical equilibrium-limited ion transfer reaction involving lime. Carbonate ions are replaced

with hydroxide ions, using calcium hydroxide in the presence of sodium sulfide ('causticizing reaction'):

$$Ca(OH)_2(aq) + Na_2CO_3(aq) \rightarrow 2\,NaOH(aq) + CaCO_3(s) \quad (1)$$

The calcium carbonate is precipitated, separated, and then reburned in a lime kiln

$$CaCO_3 + \text{heat} \rightarrow CaO + CO_2 \quad (2)$$

Slaking then closes the lime cycle (Equation 1):

$$CaO + H_2O \rightarrow Ca(OH)_2 \quad (3)$$

The main requirement for any recausticizing process in the kraft chemical recovery cycle is therefore to remove the carbonate ion from the system and replace it with the hydroxide ion in the presence of the sodium sulfide that was produced in the recovery furnace. In an attempt to alleviate the bottleneck induced by the lime cycle and circumvent the necessity of the lime kiln and associated equipment, we have developed a concept for recycling of pulping chemicals using molten salt electrochemistry at approximately 850 °C. The targeted process is a single-step electrolysis process for the molten kraft smelt. The main purpose of this process is to replace sodium carbonate (Na_2CO_3) with sodium oxide (Na_2O) in the molten smelt while not altering the sodium sulfide (Na_2S). Carbon is removed from the smelt as carbonaceous gas. The Na_2O in the postelectrolysis smelt then reacts with H_2O upon dissolving in water to form the desired NaOH. Dissolving the post electrolysis smelt therefore produces the 'white liquor' needed for the kraft process.

1.2. *Electrochemical reactions*

There is no reported work on the electrolysis of molten kraft smelt or mixtures with similar compositions. However, existing work involving electrolysis of the single components allows us to postulate possible electrochemical reactions and electrode materials for the Na_2CO_3–Na_2SO_4 system. The behaviour of sulfide ions and oxide ions will be addressed in future communications.

1.2.1. *Thermodynamics*

All standard potentials ($E°$) are with reference to the carbonate–carbon dioxide–oxygen system at 900 °C,

$$CO_3^{2-} \rightarrow CO_2 + \tfrac{1}{2}O_2 + 2\,e^- \quad E°_{900\,°C} = 0\ V \quad (4)$$

The standard potential is related to the free energy of reaction by

$$\Delta g°_{rxn} = -nFE°_{rxn} \quad (5)$$

The standard potentials are evaluated with unit activity of all species at 900 °C in the theoretical analysis and are based on the JANAF tables [4], Bureau of Mines Bulletin [5] and values provided elsewhere in the literature as cited. The operating temperature in our experiments was about 860 °C, corresponding to an increase in the standard potential by approximately 0.02 V.

1.2.2. *Sodium carbonate*

Electrochemical oxidations of molten carbonate and oxide ions have been described in sodium carbonate at 900 °C [6], in lithium–sodium carbonate at 550 °C [7] and in lithium–sodium–potassium carbonates in the range 500–733 °C [8]. These studies note the general trend for the consumption of oxide ions (Equation 6), a minor component in the smelt from thermal decomposition of carbonate,

$$O^{2-} \rightarrow \tfrac{1}{2}\,O_2 + 2\,e^- \quad E°_{900\,°C} = -0.888\ V \quad (6)$$

followed by the oxidation of the carbonate ion (Equation 4) as current density and positive potential are increased.

Possible reduction paths for Na_2CO_3 include the production of elemental sodium, sodium oxide production and carbon deposition. Davy reported the first isolation of an alkali metal by means of electrolysis in the early nineteenth century [9]. Globules of potassium and sodium were formed from molten potash and soda, respectively, when electrolysed on platina (platinum) spoons. Cathodic carbon deposition has been reported [10] at 600 °C but not at 700 °C in $(Li–Na–K)_2–CO_3$. This is predicted from the thermodynamic CO_2–C–CO equilibrium ($\Delta g°_{626.85\,°C} = 12.14$ kJ mol^{-1} and ($\Delta g°_{726.85\,°C} = -5.02$ kJ mol^{-1}). Janz and Conte also report that the primary cathodic process at 600–700 °C is alkali metal reduction:

$$M^+ + e^- \rightarrow M \quad (7)$$

where carbon or carbon monoxide is likely to be formed by one of the secondary chemical reactions between the metal and metal carbonate.

Deanhardt et al. [11] conclude that carbon is produced when electrolysing potassium carbonate in a fluoride molten salt at 500 and 700 °C. Voltammetric studies showed the alkali metal cations reduced at less negative potentials than the carbonate ions. In addition to the metal reduction (Equation 7), Ingram et al. [12] report an alternative route to the electrochemical deposition of carbon in mixed cation carbonates at 600 and 750 °C. In melts containing the Li^+ ion, carbon deposition is observed; the enhanced electrochemical activity of the carbon has been shown to arise from the occlusion of oxide ions within the deposit.

$$CO_3^{2-} + 4\,e^- \rightarrow 3\,O^{2-} + C \quad E°_{900\,°C} = -2.28\ V \quad (8)$$

Lorenz and Janz [8] predict deposition of carbon (Equation 8) in addition to the reduction evolving carbon monoxide,

$$CO_3^{2-} + 2\,e^- \rightarrow 2\,O^{2-} + CO \quad E^\circ_{900\,^\circ C} = -2.625\,V \tag{9}$$

which becomes thermodynamically favoured to Equation 8 at around 870 °C in a $(Li–Na–K)_2CO_3$ melt.

1.2.3. *Sodium sulfate*

Sulfur compounds are present in the black liquor in a range of oxidation states between sulfide and sulfate. Sequeira and Hocking [13] determined that SO_3 and O_2 are the only oxidation products in Na_2SO_4 melts at 900 °C,

$$SO_4^{2-} \rightarrow SO_3 + \tfrac{1}{2}\,O_2 + 2\,e^- \quad E^\circ_{900\,^\circ C} = +1.203\,V \tag{10}$$

In relation to hot corrosion Rapp and Goto [14] have proposed the electrolytic reduction of sodium sulfate at 927 °C through a sequence of two-electron transfers resulting in the formation of sodium sulfide and sodium oxide (Table 1).

These reactions occur at potentials considerably less negative (~0.55 V) than required for the reduction of Na^+ in the temperature range of interest; therefore the production of sodium metal (Equations 7 and 22) may be avoided. In a following report, Park and Rapp [15] present a phase stability diagram and a cyclic voltammogram for the reduction of sodium sulfate (900 °C, atmosphere of 0.1% SO_2–O_2) and confirm the overall eight electron reduction process as in Equation 15 (Table 1).

Standard potentials have not been determined for the second and third steps since thermodynamic data is not available for the sulfoxylate ion, SO_2^{2-}, although they can be combined,

$$SO_3^{2-} + 4\,e^- \rightarrow S^0 + 3\,O^{2-} \quad E^\circ_{900\,^\circ C} = -1.943\,V \tag{16}$$

where sulfur would further electrochemically reduce to sulfide (Equation 14) or chemically react with sulfide to form polysulfide,

$$\tfrac{1}{2}S_2^0 + Na_2S \leftrightarrow Na_2S_2 \quad K_{900\,^\circ C} = 1.28 \times 10^2 \tag{17}$$

Table 1. Thermodynamic standard potentials for reduction of sulfate and related ions referenced to carbonate ion oxidation (Equation 4) at 900 °C calculated from JANAF tables [4]

Reduction	$E^\circ_{900\,^\circ C}$/V	Equation
$SO_4^{2-} + 2\,e^- \rightarrow SO_3^{2-} + O^{2-}$	−1.822	11
$SO_3^{2-} + 2\,e^- \rightarrow SO_2^{2-} + O^{2-}$		12
$SO_2^{2-} + 2\,e^- \rightarrow \tfrac{1}{2}S_2^0 + 2\,O^{2-}$		13
$\tfrac{1}{2}\,S_2^0 + 2\,e^- \rightarrow S^{2-}$	−0.701	14
Overall:		
$SO_4^{2-} + 8\,e^- \rightarrow S^{2-} + 4\,O^{2-}$	−1.663	15

Sulfite, SO_3^{2-}, may play an intermediate role, yet it is not likely to be a final reaction product due to its tendency to disproportionate:

$$4\,Na_2SO_3 \leftrightarrow Na_2S + 3\,Na_2SO_4 \quad K_{900\,^\circ C} = 1.74 \times 10^9 \tag{18}$$

1.2.4. *Sodium carbonate and sodium sulfate*

Because our system has a larger concentration of carbonate than sulfate ions, and the oxidation potential for sulfate (Equation 10) lies more than a volt positive with respect to the carbonate ion discharge (Equation 4), we anticipate that the bulk oxidation will be of the carbonate ion (Equation 4). Further support for this hypothesis is presented by Flood et al. [16] who reports on the oxidative discharge of the oxide and carbonate ions in a solvent of sodium sulfate. In a mixture of Na_2CO_3 and Na_2SO_4 the bulk reduction at less negative potentials is expected to be sulfate to sulfide and oxide ions, followed by sodium carbonate reduction to sodium oxide and carbon monoxide at more negative potentials.

1.2.5. *Nickel and nickel oxide electrodes in sodium carbonate*

Nickel oxide has become the positive electrode of choice in molten carbonate fuel cells (MCFC) [17, 18, 19]. As a result we consider nickel (as the negative electrode) and nickel oxide as possible economical electrodes for our purpose. Ingram and Janz [20] have constructed a stability diagram for the nickel-ternary carbonate system at 600 °C. The literature reports the solubility of NiO in carbonate to be affected by temperature (decreasing with increasing temperature), partial pressure of CO_2 [21] and activity of Na_2O [22]. Nickel metal is stable under reducing conditions.

In summary, we will examine the electrochemical behaviour of sodium carbonate–sulfate melts under conditions similar to those of kraft smelts as a first step towards a conceptual electrochemical causticizing process. The goal is to test the feasibility of electrochemically converting the bulk of the Na_2CO_3 and Na_2SO_4 to Na_2O and Na_2S. Dissolving a sodium oxide-containing melt in water will then yield the desired sodium hydroxide. Conversion of sodium sulfate to sodium sulfide will benefit the kraft process since sodium sulfate is an inactive deadload in kraft pulping.

2. Experimental details

2.1. *Apparatus*

2.1.1. *Electrochemical cell*

A flanged Inconel reactor (20 cm i.d., 76 cm height) ('a' in Figure 1) was inserted into a top loading furnace (model 56822, Lindberg, Watertown, WI) ('b'). The temperature of the bulk molten salts in an alumina

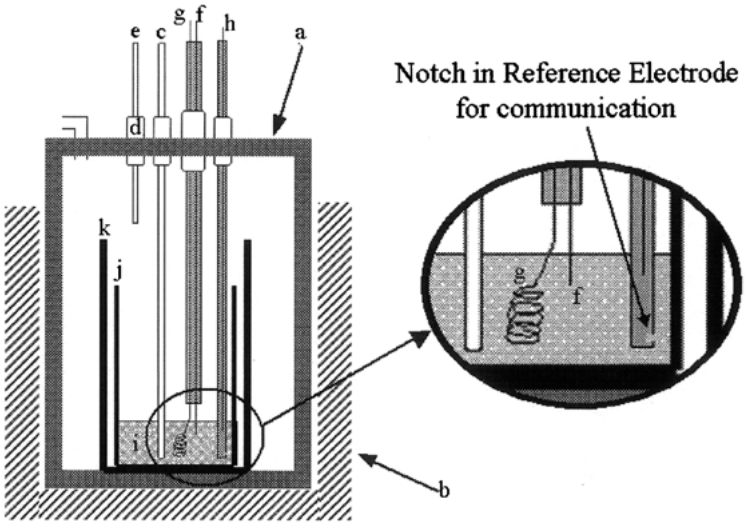

Fig. 1. Electrochemical cell overview and detail of electrodes and thermocouple in the alumina crucible.

crucible was controlled to ±5 °C as monitored by a K-type thermocouple (Omega Engineering, Stamford, CT) in a one-fourth inch round-bottom alumina well (Omega Engineering) ('c'). Multiple ports on top of the reactor were equipped with polypropylene compression fittings (Swagelok, Solon, OH) ('d') to allow height adjustment of the electrodes, the purge port (Omega Engineering) ('e') and the thermocouple well. The fittings also provided electrical isolation. The cell was operated in a three-electrode configuration, with the working electrode ('f') and counter electrode ('g') housed in a double bored alumina tube (Alfa Aesar, Ward Hill, MA; 91 cm length, dia. 0.3175 cm, 0.1 cm bore for each electrode) and a quasi-reference electrode in a separate alumina tube three centimetres away ('h'). A small hole was drilled in the bottom of the alumina tube housing the reference electrode to allow for communication with the main molten salt compartment while minimizing contamination of the reference system. The electrode materials were either gold or nickel wires (0.0254 and 0.038 cm dia., respectively, Alfa Aesar, Ward Hill, MA) attached to the potentiostat with alligator clips.

2.1.2. *Carbonate reference electrode*

The carbonate reference electrode (CRE) was similar to the one used by Andersen [23]. Air from the environment, used as the reference gas, was assumed to have a composition of 20.9% oxygen and 340 ppm carbon dioxide,

$$\mathrm{Au}\,|\,\mathrm{O_2, CO_2}\,|\,\mathrm{M_2CO_3(l)}\,|\,\text{diffusion area}\,|\,\text{electrode}$$

The reference reaction follows the dynamic equilibrium of the CRE producing zero potential at unit activity of all species, assuming reversibility, according to Equation 4, or

$$\mathrm{CO_2} + \tfrac{1}{2}\,\mathrm{O_2} + 2\,\mathrm{e^-} \rightarrow \mathrm{CO_3^{2-}} \quad E^{\circ}_{900\,^{\circ}\mathrm{C}} = 0\ \mathrm{V} \qquad (19)$$

2.2. *Materials*

Sodium carbonate and sodium sulfate (anhydrous, granular, 99.5% assay, VWR) were dried for 24 h in an oven at 115 °C. Industrial grade argon (Air Products) served as the purge gas. The molten salt mixture ('i') was contained in a flat-bottomed cylindrical alumina crucible (99.8% Al_2O_3, 8.3 cm dia., 16 cm tall, Coors Technical Ceramics, Golden, CO) ('j'). A larger diameter crucible (99.8% Al_2O_3, 10.5 cm dia., 19.4 cm tall, Coors Technical Ceramics) ('k') was used to contain the melt in the event of crucible failure.

2.3. *Procedure*

2.3.1. *Reactor set-up and heating*

Solid, granular sodium carbonate or mixtures of sodium carbonate and sodium sulfate were placed in the alumina crucible. The electrodes were inserted into the top of the reactor and lowered above the melt. The loaded alumina crucible was positioned in the bottom of the reactor before closing the reactor. The ceramic purge port was secured 20–30 cm above the material in the crucible while the sheathed thermocouple was positioned 1 cm from the bottom of the smelt crucible. The system was purged with argon (0.5–1.2 L_{STP} min^{-1}) for 3 h before heating. The electrochemical cell was heated at about 100 °C h^{-1} until the temperature reached 860 ± 5 °C.

2.3.2. *Cyclic voltammetry*

Gold or nickel wire (0.05 to 0.1 cm^{-2} submerged area in the smelt) extending 2 cm from the alumina tube ('f') and about 1.5 cm into the melt was used as the working electrode. The counter electrode was the same material as the working electrode but with at least an order of magnitude greater submerged surface area, achieved by coiling the wire ('g'). The voltammograms were IR compensated with the melt conductivity, distance be-

tween working and reference electrodes and area of the working electrode. The conductivity of the carbonate between the working and reference electrodes was measured by current interruption as 200 S m^{-1}, in good agreement with 185 S m^{-1} reported [23] for the ternary carbonate eutectic (Na–K–Li). The potential between the working and the reference electrodes was allowed to stabilize about 15 min before scanning. The voltammograms were obtained at a scan rate of 0.1 V s^{-1}. Starting from the open circuit potential the potential was scanned to predetermined values. Limits on the potential range were set to avoid excessive current densities that could compromise the stability of the electrode. Data were obtained by an EG&G (Oak Ridge, TN) model 263A potentiostat/galvanostat connected to a personal computer running National Instruments data acquisition hardware and EG&Gs M270 software.

3. Results and discussion

3.1. *Sodium carbonate on gold electrodes at 860 °C under argon purge*

3.1.1. *Bulk oxidation in sodium carbonate*

The main oxidation reaction is similar to the reference oxidation of sodium carbonate (Equation 4) on a gold working electrode under an argon purge. If activities of the components are the same and reversibility is assumed, the standard potential would be 0 V with respect to our CRE. The carbon dioxide and oxygen produced by the oxidation are expected to exhibit some reduction current (Equation 19) on the reverse scan after the potential is switched [17].

The oxidative branch of the cyclic voltammogram (two consecutive scans at 0.1 V s^{-1}) for sodium carbonate on a gold working electrode at 860 °C under an argon atmosphere is shown in Figures 2 and 3. The letter A indicates carbonate oxidation (Equation 4) and B

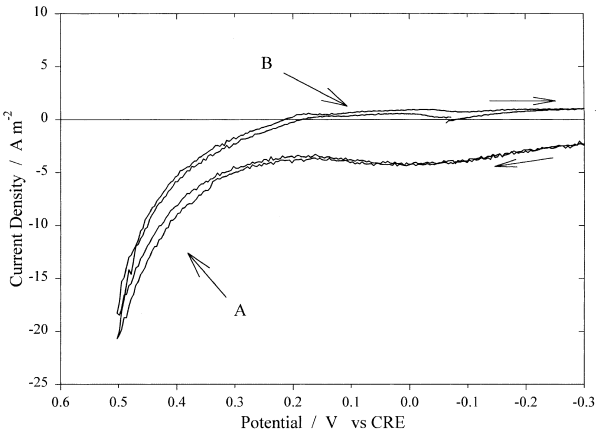

Fig. 2. Oxidation portion of a steady-state cyclic voltammogram (0.1 V s^{-1}) for Na_2CO_3 on Au under argon at 860 °C. 0.4 V shift to negative potentials due to nernstian effects between the working and the reference electrode. A indicates oxidation of carbonate and B is the rereduction of carbon dioxide and oxygen generated at A.

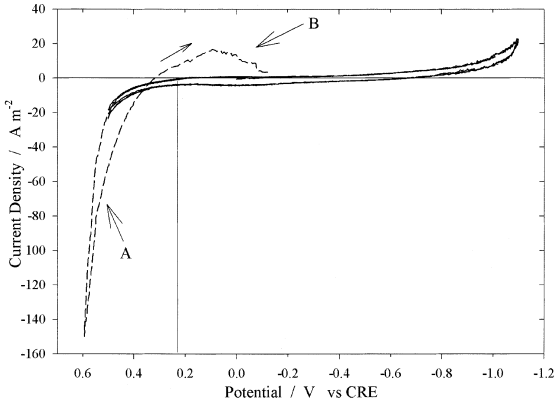

Fig. 3. Two steady-state cyclic voltammograms (0.1 V s^{-1}) with different extensions into the positive potential region demonstrate the reduction of oxidation products in Na_2CO_3 at 860 °C on Au electrodes under argon. Vertical line indicates theoretical shift attributed to nernstian effects. A indicates oxidation of carbonate and B is the rereduction of carbon dioxide and oxygen generated at A.

indicates the rereduction of product gases (Equation 19). Some oxide ions produced at the counter electrode will contribute to the current observed at A by oxidizing to produce oxygen. As a result, it appears necessary to divide the electrochemical cell in the envisioned technical process to avoid the oxidative consumption of oxide ions products.

Peak B is likely the reduction of carbon dioxide and oxygen to carbonate (Equation 19, reverse of bulk oxidation) or the reduction of oxygen to oxide ions and possible chemical reaction with carbon dioxide to reform carbonate [17, 24–26]. The positive displacement of carbonate ion oxidation from 0 V in the data (Figures 2 and 3) is attributed to the differences in CO_2 and O_2 activities between the reference electrode (air purged) and the bulk (argon purged). The resulting Nernst shift for the reference electrode is

$$-\frac{RT}{nF}\ln\left(\frac{a_{CO_3^{2-}}}{a_{CO_2}\times a_{O_2}^{1/2}}\right) = -0.0488 \times \ln\left(\frac{1}{0.209\times 0.00034^{1/2}}\right) = -0.271\ \text{V} \qquad (20)$$

where n (=2) is the number of electrons involved in the redox couple, F is the faradaic constant, R is the gas constant and T is the temperature in kelvin. When the working electrode experiences carbonate oxidation (A, Figures 2 and 3), CO_2 and O_2 are present in the ratio of 2:1. This ratio may be used to determine the Nernst shift at low current densities:

$$-\frac{RT}{nF}\ln\left(\frac{a_{CO_3^{2-}}}{a_{CO_2}\times a_{O_2}^{1/2}}\right) = -0.0488 \times \ln\left(\frac{1}{0.66\times 0.33^{1/2}}\right) = -0.047\,\text{V} \qquad (21)$$

The difference between the working electrode and the reference is expected to be +0.223 V (indicated by a

vertical line in Figures 2 and 3). It can be seen in Figure 3 that the bulk oxidation initiates at approximately this expected potential.

3.1.2. *Reduction in sodium carbonate*

The primary cathodic reaction in sodium carbonate on gold electrodes under an argon atmosphere is the reduction of sodium ions to metal [7, 8, 12].

$$Na^+ + e^- \rightarrow Na^0 \quad E^\circ_{900\,^\circ C} = -2.19\,V \qquad (22)$$

This literature suggests that at more negative potentials the secondary reaction of carbonate ions reducing to oxide ions and carbon (Equation 8) or CO (Equation 9) occurs. Andersen [23] reports a $51(O^{2-})$–$39(O_2^{2-})$–$10(1/2\ O_2^-)$ mol % split between the oxide ions at 927 °C under 1 atm oxygen in sodium carbonate; we therefore assume a variety of oxide ions will be involved in the electrochemical re-oxidations as presented in Table 2.

Cyclic voltammograms scanned at 0.1 V s^{-1} indicate multiple reductions for sodium carbonate on gold electrodes at 860 °C under an argon atmosphere (Figures 4 and 5). Figure 4 shows the steady-state scan. The dashed line in Figure 5 is a single scan overlaid onto a steady-state scan (solid) extending to less negative potentials. The span of potential between the bulk reduction (D) and bulk oxidation (A) waves indicates a window of 2.2 V. The positive potential limit shows carbonate oxidation (Equation 4) and is indicated by the letter A. Two reductions are indicated in Figure 4 (C and D); their respective reoxidations suggest anodic stripping of metal (E and F) [12]. Figure 5 indicates a different reduction at further negative potentials (G).

Table 2. Thermodynamic standard potentials for oxidation of oxide ions referenced to carbonate ion oxidation (Equation 4) at 900 °C calculated from JANAF tables [4]

	Oxidation	$E^\circ_{900\,^\circ C}$/V	Equation
Superoxide to oxygen	$O_2^- \rightarrow O_2 + 1\,e^-$	−1.06	23
Oxide to oxygen	$O^{2-} \rightarrow \frac{1}{2}O_2 + 2\,e^-$	−0.888	6
Oxide to peroxide	$2O^{2-} \rightarrow O_2^{2-} + 2\,e^-$	−0.878	24
Peroxide to oxygen	$O_2^{2-} \rightarrow O_2 + 2\,e^-$	−0.791	25
Oxide to superoxide	$2O^{2-} \rightarrow O_2^- + 3\,e^-$	−0.759	26
Peroxide to superoxide	$O_2^{2-} \rightarrow O_2^- + 1\,e^-$	−0.521	27

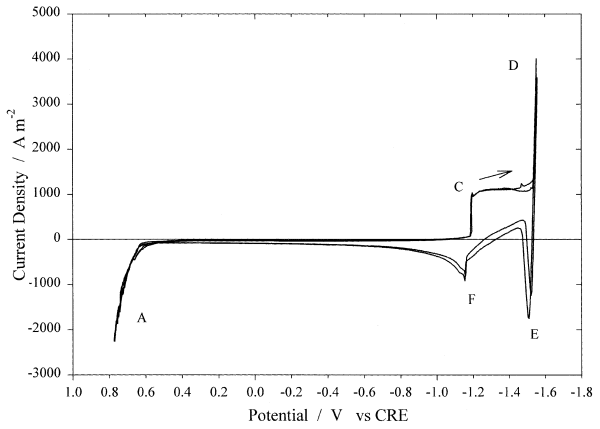

Fig. 4. Steady-state cyclic voltammograms (0.1 V s^{-1}) for Na_2CO_3 on gold at 860 °C in an argon atmosphere. C represents predeposition of sodium while D is sodium reduction. E and F are the respective oxidations of C and D. A indicates the oxidation of carbonate.

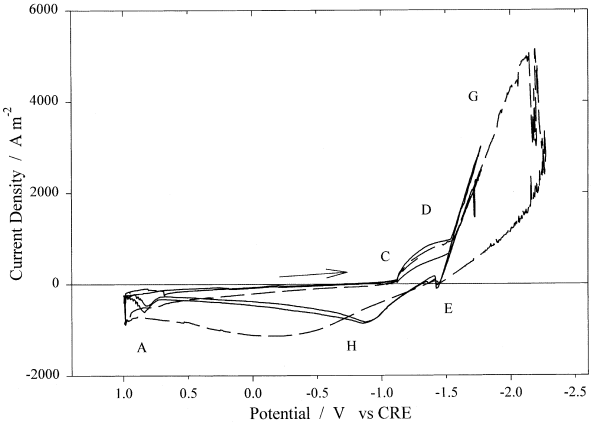

Fig. 5. Steady-state (solid) cyclic voltammograms (0.1 V s^{-1}) and an overlaid single scan (dashed line) extending to more negative potentials for Na_2CO_3 on gold under argon at 860 °C. C represents predeposition of sodium while D is sodium reduction. E and F are the respective oxidations of C and D. G represents carbonate reduction to carbon dioxide (bubbles) and oxide ions. E shows reoxidation current for sodium and H is the oxidation of the oxide ion family listed in Table 1. A indicates the start of the oxidation of carbonate.

The prewave reduction of sodium ions to sodium metal appears at −1.2 V vs CRE (C) in Figure 4; this is 0.38 V less negative than the main reduction. A similar observation has been reported by Ingram et al. [12] at 750 °C in a binary mixture of Na_2CO_3 and Li_2CO_3 where the prewave occurs 0.45 V less negative than the bulk alkali metal reduction. The main reduction is observed in Figure 4 at −1.58 V (D); the span from A to D is 2.2 V and matches the thermodynamic prediction (−2.19 V vs CRE (Equation 22)) for the reduction of sodium ions to sodium metal. Ingram et al. [12] suggest the second wave (D) is due to the production of the free metal (Equation 22). The reoxidation of the sodium metal and sodium/gold amalgamate in Figure 4 exhibits stripping peaks indicated by the waves at E and F.

At negative potentials less than −2.2 V a complex reduction is seen (Figure 5, G), where gas/vapor release is apparent as rapid fluctuations of the current. The bubbling can be due to either the vapourization of sodium metal (b.p.$_{Na}$ = 898 °C) from local Joule heating of the electrode or to the carbonate ions reducing to form carbon monoxide gas in addition to oxide ions (Equation 9). Oxidation of soluble reduction products of oxide ions (H) is seen in addition to sodium metal stripping (E) in one scan (solid line) in Figure 5. The oxidation H depends on the reduction occurring at G and is not seen when the scan is only taken to the potentials of D.

The reduction of the carbonate ion is believed to be involved since (a) the potential span between A and G is sufficiently negative (−2.28 V (Equation 8) to −2.625 V (Equation 9)), (b) the reoxidation of the cathodic products at H (Figure 5, dashed scan) no longer exhibits

the stripping peak observed in Figure 4, and (c) the extended reoxidation at H corresponds with the thermodynamic prediction for the oxidation of the oxide ions (−1.06 V through −0.521 V, (Equations 6, 23–27)). The possible involvement of carbon as a reduction intermediate or product in sodium carbonate at 900 °C in an argon atmosphere on gold electrodes has not been elucidated by this study.

3.2. *Sodium carbonate and sodium sulfate on gold electrodes at 860 °C under argon purge*

3.2.1. *Oxidations in a sodium carbonate and sodium sulfate mixture*

In a mixture of Na_2CO_3 and Na_2SO_4 the anticipated oxidation at 860 °C will be either carbonate ion oxidation to CO_2 and O_2 (Equation 4) or sulfate ion oxidation to SO_3 and O_2 (Equation 10).

A steady state cyclic voltammogram (0.1 V s^{-1}) for a mixture of sodium carbonate and sodium sulfate in a 2.36:1 molar ratio on gold electrodes under an argon atmosphere at 860 °C is presented in Figure 6.

The bulk oxidation (A, Figures 6 and 7) of the mixture occurs near the reference potential as observed in the pure sodium carbonate melt. The wave at B is observed after oxidation at A (Equation 4) on the second cycle (Figure 7) indicating the rereduction (Equation 19) of CO_2 and O_2. Sulfate ion oxidation (Equation 10) will not occur since its standard potential is 1.2 V positive of the bulk oxidation potential in these experiments. In confirmation, no sulfur containing species were detected in the off gases under bulk electrolysis conditions. Bulk experiments will be reported in the future.

3.2.2. *Reductions in a sodium carbonate and sodium sulfate mixture*

Rapp and Goto [14] initially proposed sodium sulfate reduction at 900 °C with a series of four, two-electron transfers in an atmosphere of sulfur trioxide and oxygen (Equations 11–14) where the overall reduction (Equation 15) has a thermodynamic standard potential of −1.663 V.

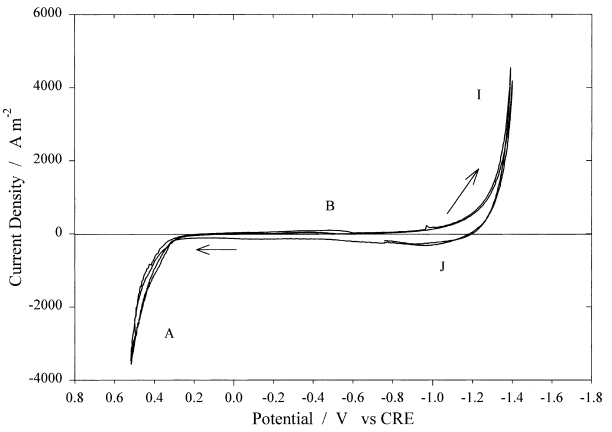

Fig. 6. Steady-state cyclic voltammogram (0.1 V s^{-1}) for Na_2CO_3 and Na_2SO_4 on gold in argon at 860 °C. A indicates carbonate oxidation with rereduction of carbon dioxide and oxygen at B. Electrochemical reduction involving sodium sulfate is indicated by I and J is the respective reoxidation.

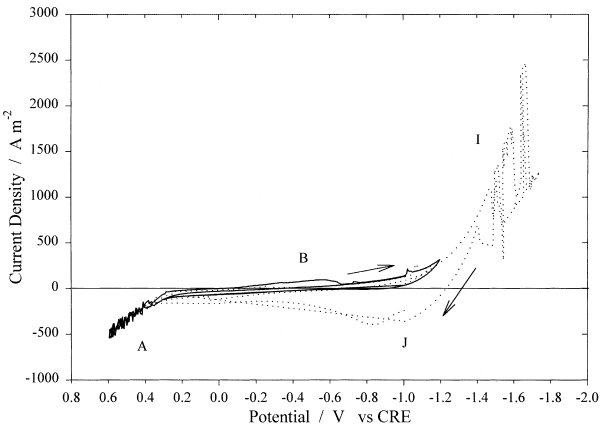

Fig. 7. Steady-state (solid) cyclic voltammogram and overlaid scan (both 0.1 V s^{-1}) extending to more negative potentials (dotted line) for Na_2CO_3 and Na_2SO_4 on gold in argon at 860 °C. A indicates carbonate oxidation with rereduction of carbon dioxide and oxygen at B. Electrochemical reduction involving Na_2SO_4 is indicated by I. J is the respective reoxidation. Gas/vapour production (bubbling) at the bulk oxidation indicates formation of CO_2 and O_2 and bubbling at the large negative potentials indicate carbonate reduction.

Two cyclic voltammograms with different potential windows (0.1 V s^{-1}, 2.36 mol:1 mol Na_2CO_3:Na_2SO_4, gold electrodes, argon purge, 860 °C) are overlaid in Figure 7. The solid scan has a shorter extension into the cathodic region (−1.2 V vs CRE) and does not show significant reoxidation of products at J; the dotted scan extending to −1.75 V vs CRE indicates gas/vapour formation (I).

Considering the observed span of −1.7 V in Figures 6 and 7 between the bulk oxidation (A) and reduction (I), the electrochemical reduction in a mixture of Na_2CO_3 and Na_2SO_4 (2.36:1 molar ratio) is sulfate ion reduction (Equation 15). A shorter span between the bulk reduction and oxidation is observed in Figures 6 and 7 than in pure sodium carbonate (Figures 4 and 5). Sodium ion reduction is not the bulk reaction as indicated by the absence of the characteristic anodic stripping peak of sodium metal in Figure 7. However, a similar oxide ion reoxidation peak (J) is observed as in pure sodium carbonate melt (H, Figure 5). In the absence of sodium metal production, the only reaction explaining the observed bubble formation is the sulfate ion reduction (Equation 15) followed by the chemical reduction of carbonate ions with the sulfoxylate ions produced according to Equation 12,

$$SO_2^{2-} + 2\,CO_3^{2-} \rightarrow SO_4^{2-} + 2\,O^{2-} + 2\,CO \qquad (28)$$

The sulfoxylate ion is a known intermediate in the reduction of sulfate ion [14] and oxidation of sulfide ion [27] while its aqueous analogues have been cited as reducing agents for dyes [28, 29]. The sulfoxylate

intermediate electrochemically reduces according to Equations 13 and 14 to produce oxide and sulfide ions. The overall combined reaction is

$$SO_4^{2-} + 2\,CO_3^{2-} + 12\,e^- \rightarrow S^{2-} + 8\,O^{2-} + 2\,CO$$
$$E^\circ_{900\,^\circ C} = -1.895\,V \quad (29)$$

This potential fits the span observed between the bulk reduction (I) and bulk oxidation (A) in Figure 7. The reoxidation wave (J, Figure 7) involves sulfide ions, the reverse of Equation 15, and the oxidations indicated in Table 2. Therefore, since both sulfide and oxide ions are prone to oxidation, a divided cell will be necessary to optimize performance. The reoxidation coulombs are approximately one half of the reduction coulombs for the scan extending to −1.75 V vs CRE. This is indicative of a nonreversible process such as gas/vapour or insoluble species formation. In summary, the overall reaction proposed (Equation 29) combines the bulk electrochemical reduction of the sulfate ion (Equation 15) with the intermediate sulfoxylate ion that chemically reacts with carbonate (Equation 29) to produce sulfate, oxide ions and carbon monoxide.

3.3. *Sodium carbonate on nickel electrodes at 860 °C under argon purge*

The scans in Figure 8 (0.1 V s^{-1}, nickel working electrode, Na_2CO_3 melt) show similar bulk reduction and oxidation characteristics as on the gold electrode (Figures 2–5) where carbonate ions are oxidized (Equation 4) (A, Figure 8), and sodium ions (Equation 22) and/or carbonate ions (Equation 9) are reduced (D/G, Figure 8). The similar electrochemical activity range indicates nickel and nickel oxide are as effective as the noble metals for electrolysis. Figure 9 is an expanded region of the reductions (K, Equations 30 and 31) and oxidation reactions (L2, Equation 32; L1, Equation 33) for nickel and nickel oxide where lower oxidation currents are observed on the initial scan.

$$NiO + 2\,e^- \leftrightarrow +Ni^0 + O^{2-} \quad E^\circ_{900\,^\circ C} = -1.50\,V \quad (30)$$

$$Ni^{3+}_{NiO} + e^- \leftrightarrow Ni^{2+}_{NiO} \quad (31)$$

$$Ni^0 + CO_3^{2-} \rightarrow NiO + CO_2 + 2\,e^- \quad E^\circ_{900\,^\circ C} = -0.697\,V \quad (32)$$

$$Ni^{2+}_{NiO} \leftrightarrow Ni^{3+}_{NiO} + e^- \quad (33)$$

A standard potential for Equation 31 is not known, yet it is reported [17] as a solid–state reaction occurring at potentials less negative than Equation 30 in the cathodic scan at 650 °C in 62/38 molar ratio Li_2CO_3/K_2CO_3 melt.

The literature [20, 17, 18, 19] reports a variety of reductions for nickel compounds in the presence of carbon dioxide and oxygen, yet Equations 30 and 31 are the dominating reductions in an argon atmosphere. The reductions are indicated by the peaks beneath K in Figures 8 and 9 and are dependent on the oxidations of L1 and L2. $NiCO_3$ is considered to play a role at lower temperatures. We are operating well above the temperature for thermal dissociation of 500 °C [30].

Nickel oxide (NiO) is formed by electrochemical oxidation and oxidation of nickel with sodium carbonate (peaks L1 (Equation 33) and L2 (Equation 32), Figures 8 and 9). The total coulombs in the peaks under K are equivalent (±1%) to peaks L1 and L2 in Figure 9; these peaks are not seen on the gold electrodes in Figures 2–5. This indicates the oxidation and reduction of nickel and nickel oxide and their reversibility in sodium carbonate at 860 °C in an argon atmosphere.

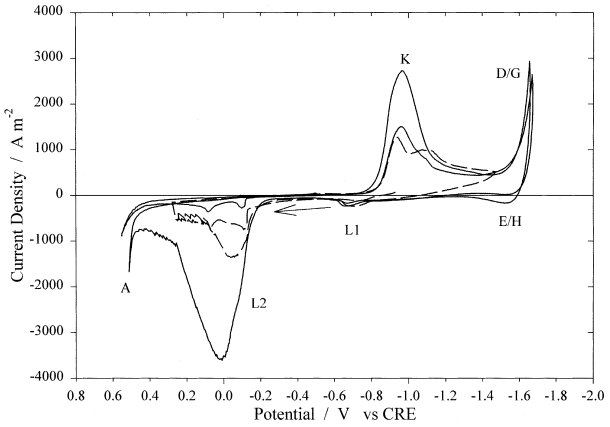

Fig. 8. Cyclic voltammograms (0.1 V s^{-1}) of Na_2CO_3 on a nickel working electrode under argon at 860 °C. Two steady-state experiments are shown (solid and dashed lines) where the initial scan had lower currents. L1 and L2 are oxidation of nickel to nickel oxide and K is the reduction of nickel oxides to nickel. A indicates carbonate ion oxidation, D/G is sodium ion and/or carbonate ion reduction where E/H is the respective oxidation.

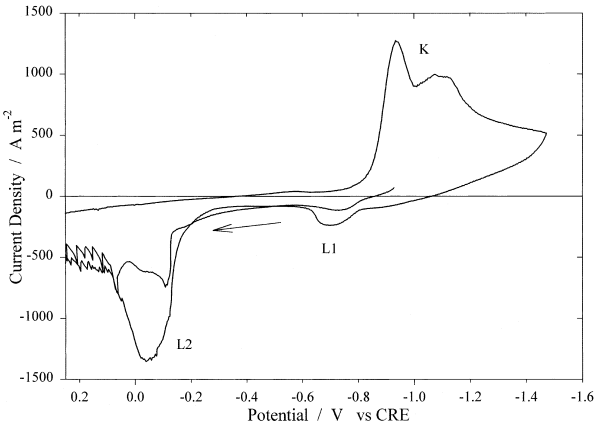

Fig. 9. Expanded scale of a steady-state cyclic voltammogram (0.1 V s^{-1}) for Na_2CO_3 on nickel working electrode under argon at 860 °C. L1 and L2 are oxidation of nickel to nickel oxide and K is the reduction of nickel oxides to nickel.

Nickel and nickel oxide were electrodes for an electrolysis experiment, preformed in a separate experimental setup, that was run for 5 h in molten sodium carbonate at 860 °C and the mass loss of the electrodes was negligible. This reinforces the CV analysis indicating nickel and nickel oxide electrodes may have promising long-term stability.

4. Summary and conclusions

The Na_2CO_3 system on gold electrodes at 860 °C in an inert atmosphere exhibits carbonate ion oxidation (Equation 4) and either sodium ion (Equation 22) or carbonate ion reduction (Equation 9) depending on electrode conditioning and the negative potential limit.

Interaction of Na_2SO_4 with Na_2CO_3 [2.36:1 molar ratio] was investigated on a gold working electrode at 860 °C. The mixture has been determined to oxidize in a similar fashion to a carbonate-only melt (Equation 4). The complimentary reductions are sulfate ions reducing to sulfide and oxide ions (Equation 15) with the sulfoxylate ion intermediate chemically reacting with carbonate (Equation 28) to give an overall reduction of sulfate and carbonate to sulfide, oxide ions and CO (Equation 29).

The nickel working electrode shows reversibility in sodium carbonate at 860 °C when considered by coulombic exchange where the two sets of reductions and oxidations are considered for nickel valence of 0, II and III. Electrolysis experiments confirm the nickel and nickel oxide electrode stability by exhibiting a negligible mass loss after five hours in Na_2CO_3 at 860 °C. This suggests nickel oxide may be a stable anode material for the pulping chemical recausticizing application, although interaction of the sulfur species will need to be considered.

Electrochemical reduction can generate sodium oxides from Na_2CO_3 and Na_2SO_4 at the target process temperature (~860 °C). These oxide ions will react with water when the molten salt is quenched, to form sodium hydroxide thereby fulfilling the main objective of the targeted technical process. Carbon is removed from the molten salt mixture by electrochemical oxidation and reduction of sodium carbonate. An additional objective is met by the sulfate ion reducing to also produce sulfide ions (a useful pulping chemical) while carbonate ion oxidation prevents sulfate ion oxidation that would lead to release of sulfur from the smelt.

From our results, it appears promising to pursue a technical process that causticizes kraft smelt by electrolysis in a divided electrochemical cell. Cyclic voltammetry suggests sodium oxides and additional sulfides (from the remaining sulfate that was not reduced to sulfide in the recovery furnace) can be formed in the melt while the carbon is released in gaseous form from mixtures of sodium carbonate and sulfate. Electrolysis experiments and the behaviour of sulfide and oxide ions as additional reactants in sodium carbonate/sulfate will be investigated in a future communication.

Acknowledgements

The authors would like to thank the United States Department of Energy (DE-FC07-97ID13547) and the Member companies of the Institute of Paper Science and Technology for their financial support.

References

1. T.M. Grace, B. Leopold and E.W. Malcolm, Alkaline Pulping, *in* M.J. Kocurek and F. Stevens (Eds), 'Pulp and Paper Manufacture' Vol. 5 (Joint Textbook Committee of the Paper Industry of the United States and Canada, Atlanta, 1991).
2. American Forest and Paper Association, 'Statistics of Paper, Paperboard and Wood Pulp', Technical Report (American Forest and Paper Association, Washington, DC, 1994).
3. T.N. Adams, W.J. Frederick, T.M. Grace, M. Hupa, K. Iisa, A.K. Jones and H. Tran, 'Kraft Recovery Boilers' (TAPPI Press, Atlanta, GA, 1997).
4. D.R. Jr. Lide (Ed.), 'Journal of Physical and Chemical Reference Data, JANAF Thermochemical Tables' (American Institute of Physics, New York, 1986).
5. K.K. Kelley and C.T. Anderson, 'Contributions to the Data on Theoretical Metallurgy: IV. Metal Carbonates – Correlations and Applications of Thermodynamic Properties' Bulletin 384 (US Department of the Interior, Bureau of Mines, Washington, DC, 1935).
6. G.G. Arkhipov, A.M. Trunov and G.K. Stepanov, *in* S.D. Pal'guev (Ed.), 'Electrochemistry of Molten and Solid Electrolytes' Vol. 2 (Consultants Bureau, New York, 1964).
7. H.E. Bartlett and K.E. Johnson, *J. Electrochem. Soc.* **114**(5) (1967) 457–461.
8. P.K. Lorenz and G.J. Janz, *Electrochim. Acta* **15** (1970) 1025–1035.
9. H. Davy, 'The Decomposition of the Fixed Alkalies and Alkaline Earths' (The University of Chicago Press, Chicago, 1906).
10. G.J. Janz and A. Conte, *Electrochim. Acta* **9** (1964) 1269–1278.
11. M.L. Deanhardt, K.H. Stern and A. Kende, *J. Electrochem. Soc.* **133**(6) (1986) 1148–1152.
12. M.D. Ingram, B. Baron and G.J. Janz, *Electrochim. Acta* **11** (1966) 1629–1639.
13. C.A.C. Sequeira and M.G. Hocking, *Electrochim. Acta* **23** (1978) 381–388.
14. R.A. Rapp and K.S. Goto, *in* J. Braunstein and J.R. Selman (Eds), Proceedings of the Second International Symposium on Molten Salts, Pittsburgh, PA, Oct. (1978), pp. 159–177.
15. C.O. Park and R.A. Rapp, *J. Electrochem. Soc.* **133**(8) (1986) 1636–1641.
16. H. Flood, T. Förland and K. Motzfeldt, *Acta Chem. Scand.* **6** (1952) 257–269.
17. J.P.T. Vossen, L. Plomp and J.H.W. de Wit, *J. Electrochem. Soc.* **141**(11) (1994) 3040–3049.
18. M.S. Yazici and J.R. Selman, *J. Electroanal. Chem.* **457** (1998) 89–97.
19. L. Qingfeng, F. Borup, I. Petrushina and N.J. Bjerrum, *J. Elelctrochem. Soc.* **146**(7) (1999) 2449–2454.
20. M.D. Ingram and G.J. Janz, *Electrochim. Acta* **10** (1965) 783–792.
21. K. Ota, S. Mitsushima, S. Kato, S. Asano, H. Yoshitake and N. Kamiya, *J. Electrochem. Soc.* **139**(3) (1992) 667–671.
22. M.L. Orfield and D.A. Shores, *J. Electrochem. Soc.* **135**(7) (1988) 1662–1668.

23. B.K. Andersen, 'Thermodynamic Properties of Molten Alkali Carbonates', Dissertation (The Technical University of Denmark, Lyngby, 1975).
24. P.K. Lorenz and G.J. Janz, *J. Electrochem. Soc.* **118**(10) (1971) 1550–1553.
25. A.J. Appleby and S. Nicholson, *J. Electroanal. Chem. Interfac. Electrochemi.* **53** (1974) 105–119.
26. M. Cassir, B. Malinowska, W. Peelen, K. Hemmes and J.H.W. de Wit, *J. Electroanal. Chem.* **433** (1997) 195–205.
27. M.A. Vairavamurthy and W. Zhou, *in* M.A. Vairavamurthy and M.A.A. Schoonen (Eds), ACS Symposium Series, 612 (Geochemical Transformations of Sedimentary Sulfur), Washington, DC, 21–25 Aug. (1994), pp. 280–292.
28. P.J. Wood, 'High-temperature vat dyeing with sodium sulfoxylate in place of sodium dithionate', XXVII Congr. Intern. Chem. Ind., Bruxelles (1954) 3, pp. 452–453.
29. V.V. Budanov and S.V. Makarov, *Khim. Khim. Tekhnol.* **31**(2) 43–46.
30. Y.A. Chang and N. Ahman, 'Thermodynamic Data on Metal Carbonates and Related Oxides' (American Institute of Mining, Metallurgical and Petroleum Engineers, New York, 1982).